General Disclaimer

One or more of the Following Statements may affect this Document

- This document has been reproduced from the best copy furnished by the organizational source. It is being released in the interest of making available as much information as possible.

- This document may contain data, which exceeds the sheet parameters. It was furnished in this condition by the organizational source and is the best copy available.

- This document may contain tone-on-tone or color graphs, charts and/or pictures, which have been reproduced in black and white.

- This document is paginated as submitted by the original source.

- Portions of this document are not fully legible due to the historical nature of some of the material. However, it is the best reproduction available from the original submission.

Produced by the NASA Center for Aerospace Information (CASI)

(NASA-TM-X-73654) HIGH STIFFNESS SEALS FOR ROTOR CRITICAL SPEED CONTROL (NASA) 25 p HC A02/MF A01 CSCL 21E

N77-32155

Unclas
G3/07 49087

NASA TECHNICAL MEMORANDUM

NASA TM X-73654

NASA TM X-73654

HIGH STIFFNESS SEALS FOR ROTOR CRITICAL SPEED CONTROL

by David P. Fleming
Lewis Research Center
Cleveland, Ohio 44135

TECHNICAL PAPER to be presented at the
Vibrations Conference
sponsored by the American Society of Mechanical Engineers
Chicago, Illinois, September 26-29, 1977

HIGH STIFFNESS SEALS FOR ROTOR CRITICAL SPEED CONTROL

by David P. Fleming

National Aeronautics and Space Administration
Lewis Research Center
Cleveland, Ohio 44135

E-9171

ABSTRACT

An annular seal is analyzed in which the inlet clearance is larger than the outlet clearance; the flow path may be either stepped or tapered. This design produces radial stiffnesses 1.7 to 14 times that of a constant-clearance seal having the same minimum clearance. When sealing high-pressure fluids, such a seal can improve rotor stability and can be used to shift troublesome critical speeds to a more suitable location.

NOMENCLATURE

A, B, E, G	coefficients given by eq. (15)
C	clearance of concentric seal
D	seal diameter
d	hydraulic diameter
e	seal eccentricity
e_r	surface roughness
F	radial restoring force
f	Fanning friction factor
H	seal clearance ratio, C_1/C_2
h	local seal clearance
I	$\int (1/h^3)dz$

STAR Category 37

J	integral defined by eq. (10)
K	seal stiffness at zero eccentricity
$\overline{K}$	dimensionless stiffness
L	seal length
M	total mass flow through seal
$\overline{M}$	dimensionless mass flow
m	local unit mass flow
N	rotational speed
N_R	resonant frequency
p	pressure
p_0	upstream stagnation pressure
V	fluid velocity
z	axial coordinate
α	angle of taper
γ	step length ratio L_1/L
ϵ	eccentricity ratio e/C_2
θ	angular coordinate
Λ	dimensionless seal length fL/C_2
ρ	fluid density

Subscripts:

b	Bernoulli
f	friction
L	at $z = L$

s	stepped
t	tapered
z	at location z
1	seal entrance or large clearance region
2	seal exit or low clearance region

INTRODUCTION

Annular pressure seals can significantly influence the dynamic behavior of rotating machinery. This is not surprising when one realizes that an annular clearance seal is essentially a journal bearing, although usually with larger clearances than normal journal bearing practice. This larger clearance reduces the hydrodynamic forces generated; however, the hydrostatic pressure difference across the seal introduces an additional means of producing seal forces. These forces vary directly with pressure difference across the seal (refs. 1 and 2) and can reach appreciable magnitudes in high-pressure seals (ref. 3). References 1 and 2 calculate stiffness and damping properties of constant-clearance annular seals.

The variation of seal radial clearance along the axis influences the forces generated. The purpose of this paper is to analyze the effects of two particular configurations: a tapered seal in which the clearance decreases uniformly from inlet to outlet, and a stepped seal in which the clearance is uniform except for a step decrease along the seal length. Radial stiffnesses and fluid flow rates will be calculated using a small eccentricity analysis, and optimum configurations derived. An example of favorable influence on rotor dynamic behavior will be presented.

ANALYSIS

The configuration to be analyzed is that of an annular clearance seal in which the clearance varies along the length of the seal. The solution will be obtained for two clearance distributions: (1) a constant taper in the axial

direction; (2) two constant clearance regions which join at a step. Solutions may also be obtained for other configurations in a straightforward manner. The two designs considered are illustrated in figure 1. The inlet clearance h_1 is, in general, larger than the outlet clearance h_2. Around the circumference the clearance is given by

$$h(z, \theta) = C(z) + C_2 \epsilon \cos \theta \tag{1}$$

When the seal is eccentric, that is, when $\epsilon \neq 0$, the fluid pressure in the seal varies in such a way that a force is generated which acts to restore concentricity. To determine this force, the pressure distribution will be calculated and integrated over the seal area. The following assumptions are employed.

1. Eccentricity is small compared with the concentric clearance, that is, $\epsilon << 1$.

2. The fluid is incompressible.

3. Rotational effects within the seal are neglected. It can be shown from the results of reference 2 that shaft rotation has a minor effect in high-pressure seals.

4. Fluid flow is one-dimensional in the axial direction; that is, circumferential flow is neglected. For high-pressure seals and small eccentricities, this is reasonably true.

5. The friction factor is constant everywhere within the seal. For turbulent flow this should introduce little error, as friction factor is a weak function of Reynolds number.

6. Flow entrance effects are negligible. For turbulent flow, entrance losses are barely detectable farther than 10 hydraulic diameters from the entrance (ref. 4).

The use of the Reynolds lubrication equation, as in a typical journal bearing, is inappropriate here because (a) the flow is usually turbulent and (b) effects of fluid inertia are significant. However, a tractable solution may be obtained

using principles developed for duct flow (ref. 4).

The axial pressure gradient due to friction is given by

$$\left(\frac{dp}{dz}\right)_f = -\frac{4f}{d}\frac{\rho V^2}{2} = -\frac{2f}{h}\frac{\rho V^2}{2} \tag{2}$$

where the hydraulic diameter $d = 2h$. The mass flow per unit width (which does not vary with z) is

$$m = \rho V h$$

Thus

$$\left(\frac{dp}{dz}\right)_f = -\frac{fm^2}{\rho h^3} \tag{3}$$

In addition to the friction pressure drop, the pressure will change due to changes in velocity (Bernoulli effect). Assuming stagnation conditions upstream of the seal,

$$\Delta p_b = -\frac{\rho V^2}{2} = -\frac{m^2}{2\rho h^2} \tag{4}$$

The local pressure is then given by the upstream pressure plus the pressure change due to velocity increase plus the friction pressure change.

$$p = p_0 - \frac{m^2}{2\rho h^2} - \frac{fm^2}{\rho}\int_0^z \frac{1}{h^3}\,dz \tag{5}$$

For a given clearance distribution, the integral may be evaluated and the pressure distribution determined.

For the tapered seal the clearance is given by

$$h = h_1 - \alpha z$$

where

$$h_1 = C_1 + e \cos \theta$$

and

$$I_{tz} = \int_0^z \frac{1}{h^3}\, dz = \frac{1}{2\alpha}\left[\frac{1}{(h_1 - \alpha z)^2} - \frac{1}{h_1^2}\right] \tag{6a}$$

For the stepped seal,

$$I_{sz} = \frac{z}{h_1^3} \qquad z \leq L$$

$$I_{sz} = \frac{L_1}{h_1^3} = \frac{z - L_1}{h_2^3} \qquad L_1 < z \leq L \tag{6b}$$

Either of equations (6) may be substituted into equation (5) and the flow found by setting $z = L$ (where $h = h_2$).

$$m^2 = \frac{(p_0 - p_L)\rho}{\frac{1}{2h_2^2} + fI_L} \tag{7}$$

The pressure within the seal is now known, and is given by

$$p = p_0 - (p_0 - p_L)\, \frac{\frac{1}{2h^2} + fI_z}{\frac{1}{2h_2^2} + fI_L} \tag{8}$$

The radial restoring force for an eccentric seal is found by integrating the pressure over the seal area, according to

$$F = -\frac{D}{2} \int_0^{2\pi} \int_0^L p \cos \theta \, dz \, d\theta \tag{9}$$

The first p_0 term in equation (8) does not contribute to the restoring force, since its integral is zero. The z integration of the remainder of equation (8) is straightforward. Defining

$$J = \int_0^L (p - p_0)\,dz \tag{10}$$

it may be readily verified that

$$J_t = \frac{p_0 - p_L}{(\alpha + f)h_1^2 - fh_2^2}\left[\left(1 + \frac{f}{\alpha}\right)h_1 h_2 (h_2 - h_1) + fLh_2^2\right] \tag{11a}$$

$$J_s = -(p_0 - p_L)\,\frac{h_1 h_2^3 L_1 + fh_2^3 L_1 (L_1 + 2L_2) + h_1^3 h_2 L_2 + fh_1^3 L_2^2}{h_1^3 h_2 + 2f\left(h_2^3 L_1 + h_1^3 L_2\right)} \tag{11b}$$

Before the integration in θ can be performed, the circumferential variation of the clearance (given by eq. (1)) must be considered. Since the eccentricity has been assumed small, any terms containing the square or higher powers of ϵ will be neglected. Equation (1) is now substituted into equation (11), and terms collected according to the power of ϵ contained. Equation (11) then becomes, with ϵ^2 and higher order terms omitted,

$$J = -(p_0 - p_L)L\left[\frac{A + B\epsilon\cos\theta}{E + G\epsilon\cos\theta}\right] \tag{12}$$

The restoring force F is given by

$$F = \frac{1}{2}(p_0 - p_L)LD\int_0^{2\pi} \frac{A + B\epsilon\cos\theta}{E + G\epsilon\cos\theta}\cos\theta\,d\theta \tag{13}$$

Expressions somewhat simpler to integrate than equation (13) may be obtained if the stiffness at zero eccentricity is calculated instead of the force.

$$K = \lim_{\epsilon \to 0} \frac{F}{C_2 \epsilon} = \frac{LD}{2C_2 E^2} (p_0 - p_L) \lim_{\epsilon \to 0} \int_0^{2\pi} (A + B\epsilon \cos\theta)(E - G\epsilon \cos\theta)\cos\theta \, d\theta \tag{14}$$

where, for small ϵ,

$$\frac{1}{E + G\epsilon \cos\theta} \sim \frac{1}{E^2} (E - G\epsilon \cos\theta)$$

The constants A, B, E, and G are given by

$$\left.\begin{aligned}
A_t &= H(H + \Lambda) \\
B_t &= H + A_t \\
E_t &= H\left[H^2 + \Lambda(H + 1)\right] \\
G_t &= 2A_t \\
A_s &= H\gamma + \Lambda\gamma(2 - \gamma) + \Lambda(1 - \gamma)^2 H^3 + (1 - \gamma)H^3 \\
B_s &= \gamma(3H + 1) + 3\Lambda\left[1 + (1 - \gamma)^2 (H^2 - 1)\right] + (1 - \gamma)H^2 (H + 3) \\
E_s &= H^3 + 2\Lambda\left[\gamma + (1 - \gamma)H^3\right] \\
G_s &= H^2 (H + 3) + 6\Lambda\left[\gamma + (1 - \gamma)H^2\right]
\end{aligned}\right\} \tag{15}$$

where

$$H = C_1/C_2; \ \Lambda = fL/C_2; \text{ and } \gamma = L_1/L$$

It is well known that $\int_0^{2\pi} \cos^n \theta \, d\theta = 0$ for any odd n and that $\int_0^{2\pi} \cos^2 \theta \, d\theta = \pi$. Thus, equation (14) becomes

$$K = \frac{(p_0 - p_L)LD}{C_2} \frac{\pi}{2E^2} (BE - AG) \tag{16}$$

It may be noted that equation (16) agrees with the results of reference 1 when $H = 1$ and the present assumptions are applied to the analysis of reference 1.

It is convenient to present results for a non-dimensional stiffness $\overline{K}$ where

$$K = \frac{KC_2}{(p_0 - p_L)LD} = \frac{\pi}{2E^2} (BE - AG) \tag{17}$$

Seal leakage flow may also be expressed in dimensionless terms. The total (dimensional) mass flow is denoted by M where

$$M = \int_0^{2\pi} \frac{mD}{2} \, d\theta \tag{18}$$

For the concentric seal,

$$M = \pi Dm \tag{19}$$

The dimensionless mass flow, from equations (6), (7), (15), and (19) is

$$\overline{M} = \frac{M}{\pi DC_2 \sqrt{(p_0 - p_L)\rho}} = \sqrt{\frac{2H^3}{E}} \tag{20}$$

RESULTS

The preceding expressions have been used to optimize the seal clearance ratio H and (for stepped seals) the step location γ. The optimization was carried out in two ways: first to maximize the seal stiffness K, and next to maximize the ratio of stiffness to flow rate. The latter optimization yielded stiffnesses only slightly lower than maximum, while reducing the leakage flow. The optimization technique was similar to that employed in reference 5, and utilizes the Newton-Raphson method.

Results are presented as functions of the dimensionless seal length $\Lambda = fL/C_2$. Figure 2 shows optimum clearance ratio for the tapered seal, and figure 3 for the stepped seal. For both seals, the optimum clearance ratio is higher for maximum K than for maximum K/M. The two values converge at low values of seal length. It can easily be shown that as seal length approaches zero, the optimum clearance ratio approaches 2 for the tapered seal and 1.5 for the stepped seal. The same value of H maximizes both K and K/M for very short seals.

The clearance ratio for stepped seals exhibits some unusual behavior which can be understood better by also considering the results for optimum step length $\gamma = L_1/L$, figure 4. The optimum step length became 1 for low seal lengths. This means that the large-clearance portion of the seal extended throughout the entire seal length with an annular orifice at the outlet. $\gamma = 1$ is, of course, the upper bound for step length, and when the optimum step length is 1 there is essentially only one parameter remaining to optimize: H. Thus, this is a different regime of the solution than when γ can vary freely. The cusps in the curves of figure 3 occur where the two solution regimes meet.

A step length of 1 would not be a practical design. Thus, a second optimization was performed in which γ was arbitrarily limited to 0.8. This became the optimum value for the entire range of seal lengths considered when maximizing K; for maximum K/M, $\gamma = 0.8$ is optimum only up to $\Lambda = 0.6$. Figure 3 shows that the optimum clearance ratio is lower when step length is restricted.

Stiffness results. - Figures 5 and 6 illustrate the stiffnesses achieved with optimum tapered and stepped seals. On both figures, the stiffness of a straight seal with the same minimum clearance (calculated by setting $H = 1$) is also plotted. Figure 5, for a tapered seal, shows that the optimum seal stiffness is always at least 70 percent greater than that of a straight seal. The stiffness

gain with the tapered seal is much greater over most of the range of seal lengths. Dimensionless stiffness drops as length increases. However, the drop is gradual enough that greater dimensional stiffness can always be obtained by making the seal longer.

Figure 6, for stepped seals, has cusps and branches in its curves corresponding to those in figures 3 and 4. A comparison of figures 5 and 6 shows that the optimum stepped seal is always stiffer than the optimum tapered seal, if the step length is allowed to vary freely. This is to be expected, since, in the stepped seal, two parameters may be varied (clearance ratio and step length) versus only one (clearance ratio) in the tapered seal. When the step length is restricted to a maximum of 0.3, however, the optimum tapered seal is stiffer for seal length $\Lambda < 0.5$. The stiffness of a stepped seal varies from 1.7 to 14 times that of a similarly dimensioned straight seal, over the range of seal lengths investigated.

Flow rates. - Flow rates through tapered seals are shown in figure 7 and through stepped seals in figure 8. The flow through a straight seal is shown for comparison in both figures. Flow through either tapered or stepped seals is only moderately higher than through straight seals. The relative increase in flow through high stiffness seals compared to straight seals rises with increasing seal length and reaches approximately 60 percent for the longest seals investigated.

A comparison of figures 7 and 8 shows that, when K/M is maximized, the flow rates are nearly identical for tapered and stepped seals. If only K is maximized, and the step length allowed to vary freely, the stepped seal allows a noticeably higher flow.

Effect of variable friction factor. - The seal clearance changes appreciably from one end of the seal to the other. If this change produces a variation in friction factor through the seal, then results calculated assuming a constant

friction factor could be in error. Two flow regimes need to be considered. In the first, that of laminar and transition-turbulent flow, friction factor depends primarily on Reynolds number. In a channel, which the seal flow passage is assumed to be, Reynolds number does not vary as long as the unit mass flow rate, density, and viscosity are constant. Since these conditions have been assumed, Reynolds number, and hence friction factor, do not vary along the length of the seal.

The second flow regime is that of fully turbulent, or inertial flow. For Reynolds numbers sufficiently high, friction factor depends only on the relative roughness of the flow bounding surfaces (ref. 4). An expression relating friction factor to relative roughness is presented in reference 4.

$$\frac{1}{\sqrt{f}} = 4 \log_{10} \frac{d}{e_r} + 2.28$$

This expression is rather cumbersome. However, a good approximation is

$$f = 0.036 \left(\frac{d}{e_r} \right)^{-0.29}$$

For the stepped seal, the friction factors for the two regions are then related by

$$f_2 = f_1 \, H^{0.29}$$

The results of the ANALYSIS section are readily modified to accept different friction factors for the two seal sections. This was done, and the optimization procedure carried out. Optimum seal parameters, as well as stiffness and flow rate varied no more than 3 percent from the constant friction factor case. Thus very little accuracy is lost by assuming a constant friction factor.

EFFECT ON ROTOR BEHAVIOR

The rotor considered in this example is from the space shuttle main engine high-pressure fuel turbopump. Figure 9 shows the rotor. Three centrifugal pump stages and two axial turbine stages are all between the ball bearing supports. The bearing span is 580 millimeters; the rotor weighs 56 kilograms (ref. 6). Annular seals are between the pump stages. The fluid pumped is liquid hydrogen; pressure difference across each seal varies approximately as the square of the rotor speed and is 136 bar at the design speed of 37 000 rpm (ref. 7). Seal diameter is 76 millimeters; length, 43 millimeters; and radial clearance, 0.13 millimeter.

Critical speeds with original straight seals. With these dimensions and pressures, the flow is fully turbulent; thus the friction factor depends only on the relative roughness. For a surface roughness of 0.8 micrometer, which is a common machining specification, the relative roughness d/e_r is 300 and the friction factor 0.007. The dimensionless seal length Λ is then 2.4. From figure 6 for a smooth seal, $\overline{K} = 0.11$.

Critical speeds for the rotor were calculated, using a critical speed computer program which allowed bearing stiffness (in this case, seal stiffness) to vary with rotor speed (the program was the same as that used in ref. 6). The first and second critical speeds were found to be 9250 and 17 970 rpm, with ball bearing support flexure stiffness of 30 MN/m. Rotor mode shapes are shown in figure 10. Since the normal speed range of this pump is from 22 000 to 37 400 rpm, at first glance the critical speeds seem well disposed. As the rotor is lightly damped, however, it is susceptible to various instabilities in which the exciting forces often occur at a frequency half or less that of the rotor speed. An example of this type of excitation is unbalanced turbine (Alford) forces (ref. 8). Thus it is desirable that any resonance occur at a frequency more than half the rotor speed.

High stiffness seals. - The first critical speed is obviously the one that needs the largest increase. Figure 10 shows that at this critical speed, amplitudes are quite high at the seal locations. Thus increased seal stiffness should result in an increased critical speed. To investigate the effectiveness of high stiffness seals, we will assume that the existing straight seals will be replaced by stepped seals optimized to maximize K/M. The present overall seal dimensions and minimum clearance will be retained.

The dimensionless seal length is thus the same as calculated for the straight seal; $\Lambda = 2.4$. From figure 3, the optimum clearance ratio is $H = 1.59$. From figure 4, the optimum step length is $\gamma = 0.70$. Figure 6 shows the stiffness $\overline{K}$ to be 0.29, or nearly three times the stiffness of the straight seal. With the stepped seals, the first two critical speeds are 10 060 and 20 190 rpm. Thus the first and second critical speeds have increased 9 and 12 percent, respectively.

The second critical speed is now more than half the design speed. However, the first critical speed is still less than one-third of the design speed. At this point, it is necessary to consider the difference between a critical speed and a resonant frequency for a particular operating condition. By definition, a critical speed occurs when the operating speed of the rotor coincides with one of its resonant frequencies. If the bearing and seal stiffnesses are invariant with speed, and gyroscopic inertia is neglected, then the resonant frequencies are also invariant. For the example considered, however, the seal stiffness increases as the square of the speed (because of the increase in pump pressure rise); the rotor also has a large polar moment of inertia. Thus the resonant frequencies will vary with rotor speed. In order to investigate the effect of speed on resonant frequency, the critical speed computer program was modified to calculate resonances rather than critical speeds; the results are shown in figure 11.

The first two resonant frequencies both increase with speed. Critical speeds occur where the resonant frequency curves intersect the synchronous line ($N_R = N$). The half-synchronous line, $N_R = N/2$ is also shown; to meet our goal, the first resonance line should be above the half-synchronous line throughout the operating speed range. As figure 11 shows, this does not occur: rotor resonant frequency is less than one-half synchronous frequency for rotational speeds greater than 27 500 rpm. Thus, simple replacement of straight seals by similarly-dimensioned high-stiffness seals affords some improvement but does not meet our goal in this example. Additional means to increase the first resonant frequency include (1) changing the stiffness of the ball bearing support flexures; (2) increasing the seal length or diameter (stiffness is proportional to seal area). However, investigation of these effects is beyond the scope of this paper. Stiffening the rotor is likely to have only a small effect, as rotor bending is very slight with stiff seals at high speeds.

CONCLUDING REMARKS

An analysis has been presented to calculate the radial stiffness of annular seals whose clearance varies in the flow direction. Seal parameters were optimized, and results presented for seals with (1) a uniform taper in the flow direction; (2) two constant-clearance regions which meet at a step. Over the range of dimensionless seal lengths investigated, the optimized seal stiffness ranged from 1.7 to 14 times that of a similarly-dimensioed straight seal. High-stiffness seals can be used to raise critical and resonant speeds of rotors, thereby improving rotor response characteristics in some cases.

REFERENCES

1. Black, H. F.: Effects of Hydraulic Forces in Annular Pressure Seals on the Vibration of Centrifugal Pump Rotors. J. Mechanical Engineering Science, vol. 11, no. 2, 1969, pp. 206-213.

2. Black, H. F.; and Jenssen, D. N.: Dynamic Hybrid Bearing Characteristics of Annular Controlled Leakage Seals. Proc. Instn. Mech. Eng., vol. 184, part 3N, 1969-1970, pp. 92-100.

3. Gunter, E. J.; Li, D. F.; Allaire, P. E.; and Barrett, L. E.: The Dynamic Analysis of the Space Shuttle Main Engine High-Pressure Fuel Turbopump. Part I - Critical Speed Analysis. University of Virginia Report UVA/528140/ME76/102, 1976.

4. Knudsen, J. G.; and Katz, D. L.: Fluid Dynamics and Heat Transfer. McGraw-Hill, 1958.

5. Hamrock, B. J.; and Fleming, D. P.: Optimization of Self-Acting Herringbone Grooved Journal Bearings for Maximum Radial Load Capacity. Proceedings of Fifth Gas Bearing Symposium, University of Southampton, 1971.

6. Childs, D. W.: Two Jeffcott-Based Modal Simulation Models for Flexible Rotating Equipment. J. Eng. for Industry, vol. 97, 1975, pp. 1000-1014.

7. Gunter, E. J.; Allaire, P. E.; and Barrett, L. E.: Interim Report on the Dynamic Analysis of the Space Shuttle Main Engine High-Pressure Fuel Turbopump. University of Virginia Report ME-4012-101-76, 1976.

8. Alford, J. S.: Protecting Turbomachinery from Self-Excited Rotor Whirl. J. Eng. for Power, vol. 87, 1965, pp. 333-344.

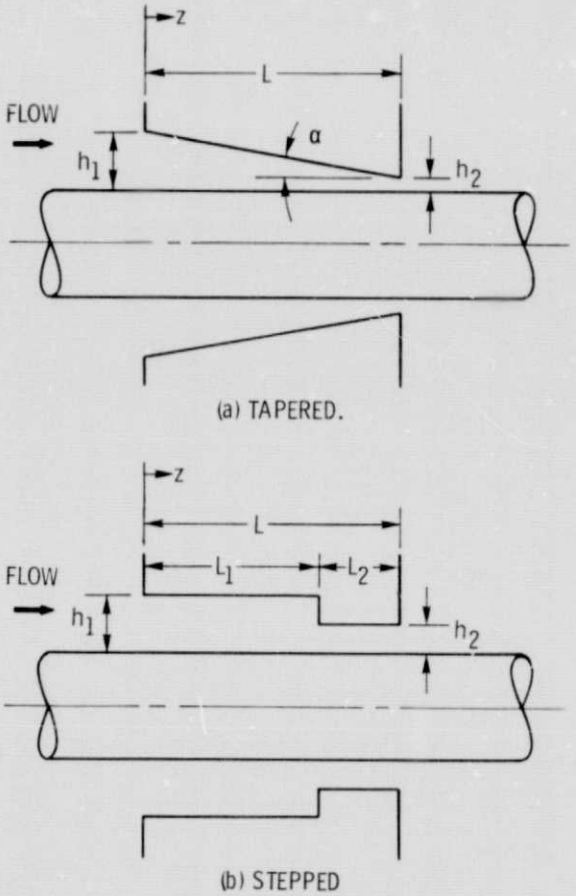

Figure 1. - Tapered and stepped annular seals.

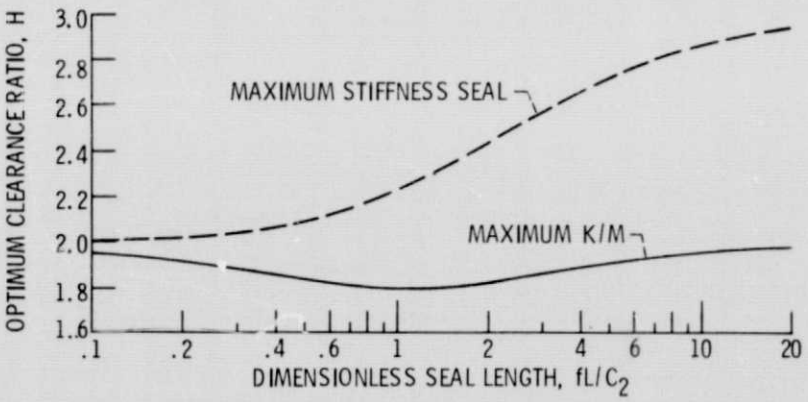

Figure 2. - Optimum clearance ratio of tapered seal.

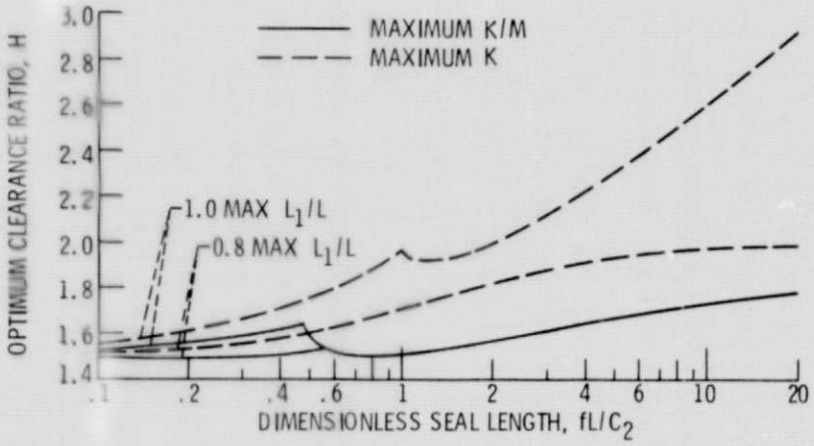

Figure 3. - Optimum clearance ratio for stepped seal.

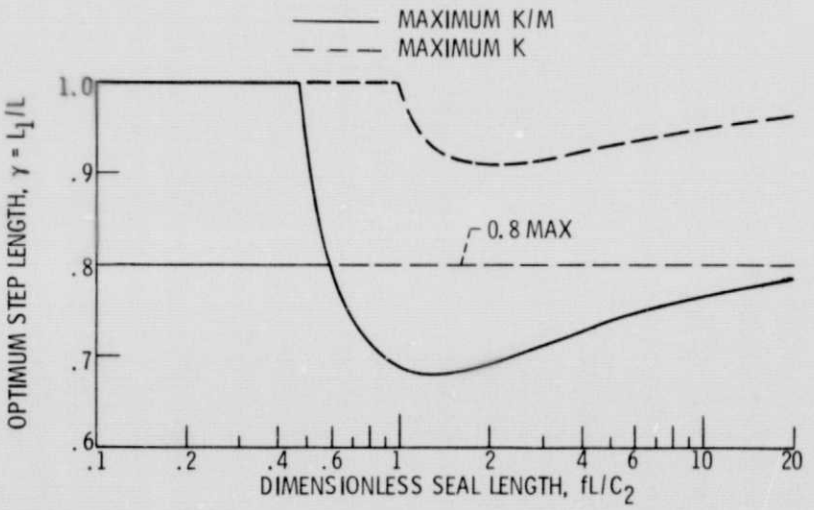

Figure 4. - Optimum step length for stepped seal.

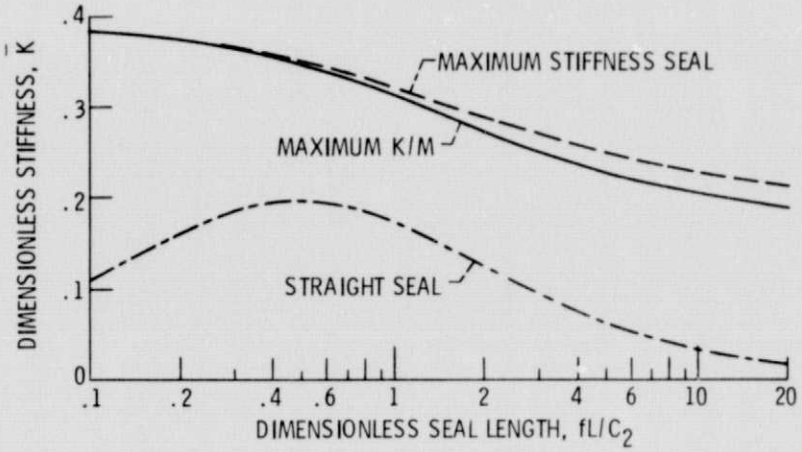

Figure 5. - Stiffness of tapered and straight seals.

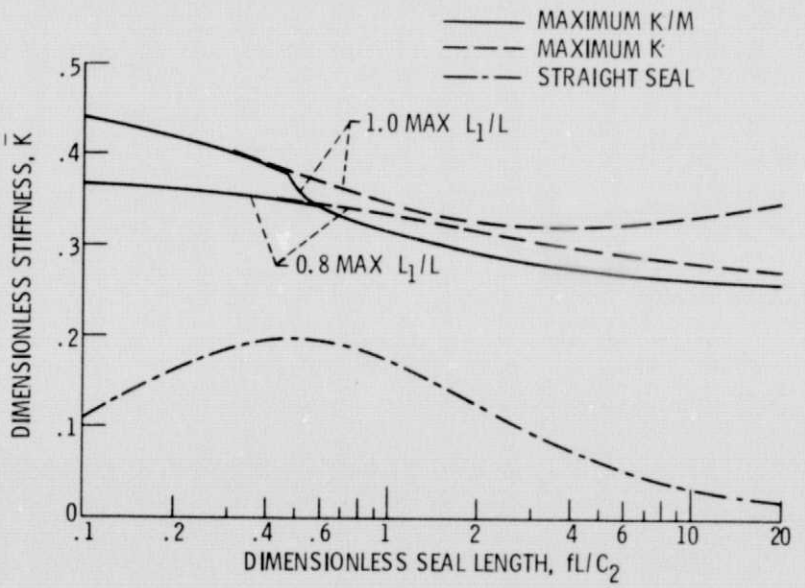

Figure 6. - Stiffness of stepped and straight seals.

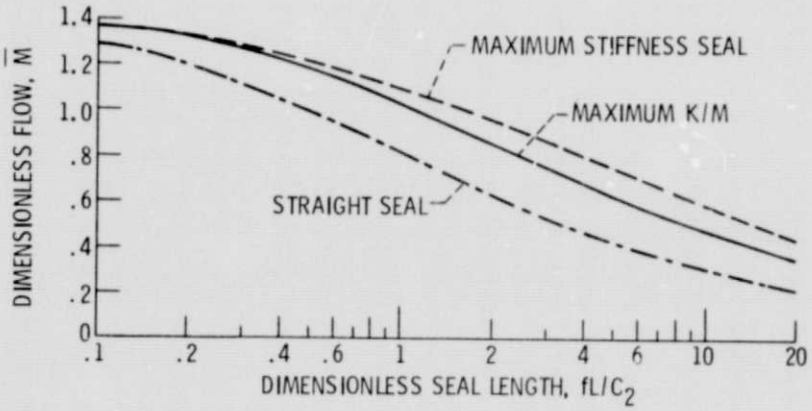

Figure 7. - Flow through tapered and straight seals.

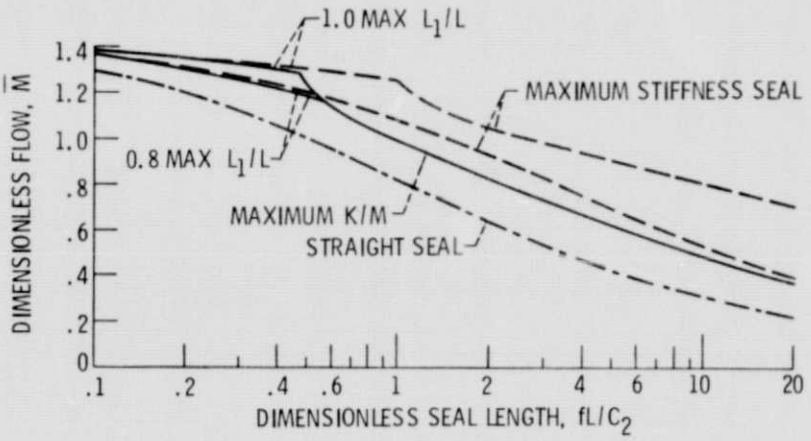

Figure 8. - Flow through stepped and straight seals.

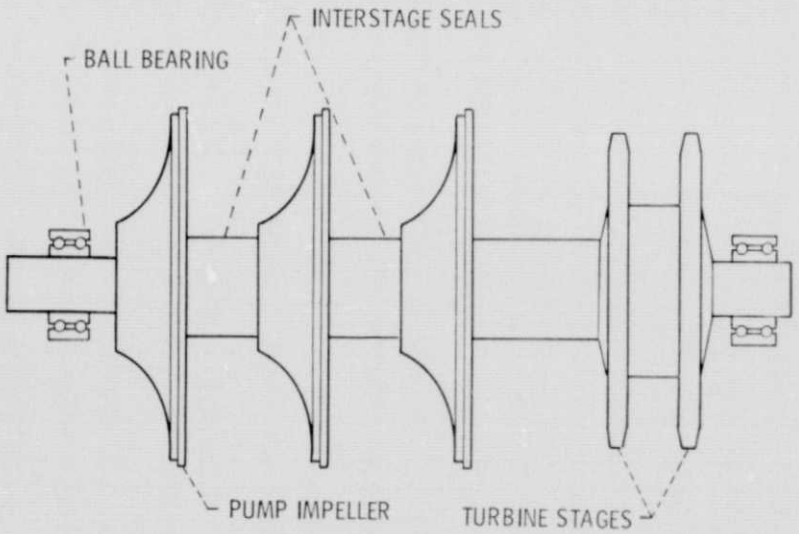

Figure 9. - Turbopump rotor.

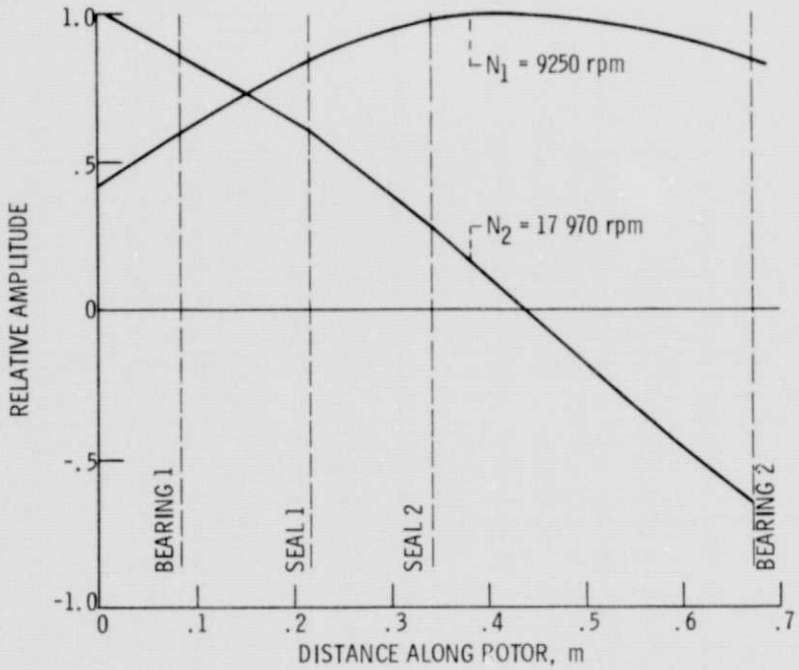

Figure 10. - Critical speed mode shapes with straight seals.

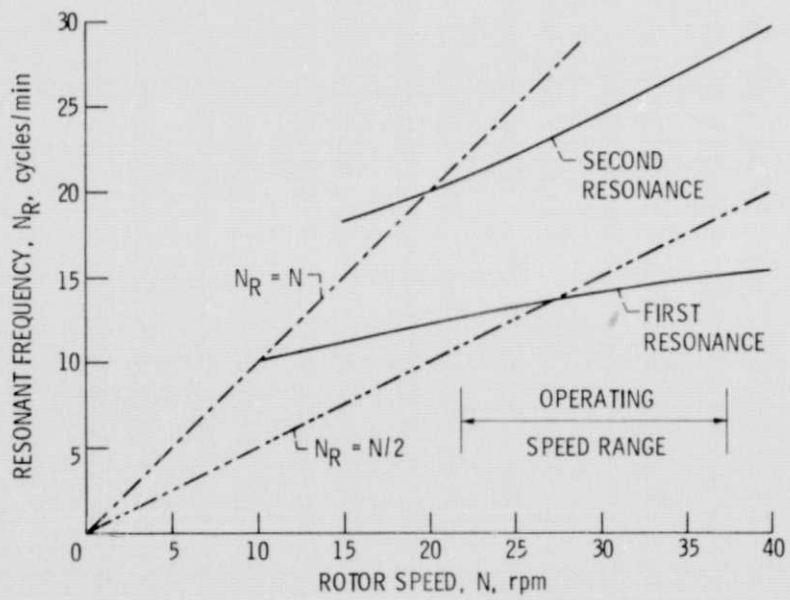

Figure 11. - Rotor resonant frequencies with optimum stepped seals.

NASA-Lewis